Dear. Referee #3

We uploaded response letter for the comments of all reviewer and revised manuscript entitled, "Retrieval pseudo BRDF-adjusted surface reflectance at 440 nm from Geostationary Environmental Monitoring Spectrometer (GEMS)".

All comments of reviewers were seriously touched by authors and answered in response letter. We tried our responses can satisfy all reviewers, and our manuscript has been more improved by your advice.

The line numbers written in this response are based on the Author's tracked changed file.

Comments and Suggestions for Authors as follows (Referee 3):

1. Some words are rarely used in the algorithm fields. The algorithm is just estimation and guessed values from several assumptions. Therefore, 'calculation' is rarely used. In addition, 'outputs' in section 2.2 is also not frequently used for the retrieval products, and 'generation' in section 3.3 is also rarely used. Please check the word related to the retrieval and retrieved dataset explanations and correct it.

➔ Thank you very much for your insightful feedback. I largely agree with your observation that certain words are rarely used in the context of algorithm fields. Specifically, terms like "generation" and "output" are indeed infrequently used when compared to other studies. However, in research papers related to surface reflectance and albedo, the term "calculation" is commonly employed. Consequently, I have made changes to all instances of "generation" and "output" throughout the text. I have also revised some instances of "calculation" where it could potentially cause confusion.

All instances of the word "output" in the text have been changed to "product".

Below is the attached text with the revised parts other than the relevant parts.The modified parts are as follows: (The previously written parts are in blue and italics, deleted parts are blue and ~~solid lines~~, and the newly added/replaced parts are in red and italics.)

(Line 25-28; In Section 1. Introduction)

In the retrieval ~~calculation~~ of surface reflectance, aerosol optical depth (AOD) and atmospheric gas products (such as ozone, total precipitable water (TPW), nitrogen dioxide (NO2), etc.) are fundamental parameters. Simultaneously, surface reflectance is crucial for the retrieval ~~calculation~~ of these atmospheric constituents and forms an essential component of their product ~~output~~.

(Line 255; Change the section title)

(Before the change)
*3.3. GEMS LER **generation***

(After the change)
*3.3. GEMS LER **assumption***

2. P1 L19: land surface reflectance is essential to the satellite remote sensing, but the surface signal is negligible to the 'ground' remote sensing. Therefore, please change the 'remote-sensing' to 'satellite remote sensing'. Also, many points in the manuscript have similar word using. Please correct it

➔ Thank you very much for your insightful feedback. All parts related to the comment have been edited.

Below, we have included the revised text for your review. The modified parts are as follows: (The previously written parts are in blue and italics, and the newly added/replaced parts are in red and italics.)

(In Abstract)
In satellite remote sensing applications, enhancing the precision of level 2 (L2) algorithms relies heavily on the accurate estimation of the surface reflectance across the ultraviolet (UV) to visible (VIS) spectrum.

(In Abstract)
These findings present a promising avenue for enhancing the accuracy of surface reflectance retrieval from hyperspectral satellite data, thereby advancing the practical applications of satellite remote sensing algorithms.

(Line 17-19; In Section 1. Introduction)
Because surface reflectance is utilized in remote- sensing systems to derive various geophysical, chemical, and biological variables (Veefkind et al., 2006; Noguchi et al., 2014), accurate satellite observations of land surface reflectance are essential for developing accurate satellite remote-sensing algorithms.

(Line 180-181; In Section 3.1. Atmospheric correction)
Atmospheric correction plays a pivotal role in satellite remote sensing by rectifying distortions caused by atmospheric effects, which can vary based on different geometries and atmospheric conditions.

(Line 221-222; In Section 3.2. BSR retrieval through BRDF modeling)
Consequently, semi-empirical BRDF models are widely employed in satellite remote sensing.

3. P2 L32-L41: From this manuscript, all the satellite algorithms are based on the minimum reflectance technique. However, it is doubtful that the minimum reflectance technique is one of the method for the surface reflectance retrieval. In addition, the GOME and OMI climatological surface reflectance data is partly different to identify the maximized surface signals. The detailed previous retrieval algorithms and other reflectance identification techniques are required.

➔ The LER (Lambertian Equivalent Reflectivity) algorithm we are most familiar with is a surface reflectance calculated based on the minimum reflectance technique. The minimum reflectance technique, used by many satellite algorithms, identifies the lowest reflectance value observed over a given period of time, assumed to represent clear sky conditions. The method is simple and often effective in areas with low reflectance variability, such as over the ocean or over stable land surfaces.

However, this method has limitations and is not universally accepted as the best method for all surface types. For example, in areas with high surface reflectance variability, such as deserts, snow-covered areas, or vegetated areas, the minimum value may not accurately represent typical surface conditions, and in areas where occasional low reflectance occurs due to temporary clouds or shadows, the reflectance may not reflect the true surface properties.

Therefore, the GOME-2 LER product generates an output called “MODE-LER”, which is available in addition to the more familiar “MIN-LER” method of selecting the minimum reflectance. Instead of selecting the minimum value that occurred during the synthesis period, the MODE-LER method adopts the most frequently occurring reflectance. This can provide a more representative measure of typical surface reflectance, especially in areas where surface conditions are highly variable.

This approach suggests that applying the minimum reflectance technique to calculate surface reflectance is limited in its ability to account for the anisotropic reflectance properties of the ground surface. However, the MODE-LER method is also a climatological dataset and is limited in its ability to parameterize all of the anisotropic reflectance properties of the ground surface, which are changing in real time. Therefore, in this study, a more realistic surface reflectance simulation was performed based on the BRDF model.

However, as the reviewer mentioned, there are several methods to calculate the reflectance of the land surface other than the minimum reflectance method in the OMI and GOME-2 satellite in situ algorithms, so we have added a reference to this in the text.

Below, we have have attached the added text for your review. The modified parts are as follows: (The previously written parts are in blue and italics, and the newly added/replaced parts are in red and italics.)

(Line 32-47; In Section 1. Introduction)

Most satellite algorithms that focus on observing the UV-VIS region, such as the Total Ozone Mapping Spectrometer (TOMS) (Herman and Celarier, 1997), Global Ozone Monitoring Experiment (GOME) (Koelemeijer et al., 2003), and Ozone Monitoring Instrument (OMI) (Kleipool et al., 2008) produce a priori surface reflectance products called Lambertian equivalent reflectance (LER). The LER archive is a climatology database calculated using the minimum reflectance method under the assumption of a Lambertian surface. The minimum reflectance technique uses the lowest observed ground reflectance for the same pixel within the compositing period. This technique assumes that the minimum value of the surface reflectance generated during the synthesis period minimizes the effects of the atmosphere and clouds, and adopts it as a stable value in a clear sky. This method has the advantage of being simple to implement, but has a limitation in that it cannot consider realistic surface reflection properties and can easily underestimate the actual surface reflectance. Occasionally, overcalculations can occur because of a failure to reflect the characteristics of changes in the indicators in real time. Therefore, to idetify more realistic surface signal, the GOME-2 (Tilstra et al., 2017) LER products have introduced the "MODE-LER" method alongside the "MIN-LER" approach. While the MIN-LER method selects the minimum reflectance observed during the synthesis period as well known, the MODE-LER method identifies the most frequently occurring reflectance value. This approach provides a more representative measure of typical surface reflectance, especially in regions with highly variable surface conditions. Although the MODE-LER method offers improvements rather than minimum reflectacne method, it remains a climatological dataset and cannot fully parameterize the anisotropic reflectance properties of surfaces, which change in real time.

4. P2 L42-58: For the Level 2 scientific product explanation, the author needs to include the references, such as ATBDs or papers of AMF errors.

➔ We recognized that there was a lack of references, and we appreciate your assistance. An additional paper was cited that emphasized the importance of considering the anisotropic nature of surface reflectivity in each Level 2 output algorithm (such as AOD, HCHO, NO2 and SO2). Additionally, to highlight the significance of the aspects explained directly in the paper, previously indirect references were changed to direct mentions.

The corrections are listed below: The modified parts are as follows: (The previously written parts are in blue and italics, and the newly added/replaced parts are in red and italics.)

(In Line 48-50; In Section 1. Introduction)

*Under- and over-estimated surface reflectance arising from neglecting surface anisotropy can significantly compromise the accuracy of other satellite-derived products such as AOD (**Kaufman et al., 1997**), formaldehyde (HCHO) (**De Smedt et al., 2018; Howlett et al., 2023**), NO2 and SO2 (**Leitão et al., 2010; McLinden et al., 2014**).*

(In Line 50-53; In Section 1. Introduction)

*For instance, an underestimated surface reflectance may result in an overestimation of the AOD (**Mei et al., 2014**), affecting the accuracy of aerosol concentration estimate. Conversly, if the surface reflectance is overestimated, the opposite effects would occur (**Chen et al., 2021; Wang et al.,2019**).*

(In Line 53-61; In Section 1. Introduction)

(Before the change)

Based on prior studies, the variation of the surface reflectance 0.05 in the blue channel can lead underestimation of approximately -0.17 in the range where the AOD is less than 0.4 (Li et al., 2012). Additionally, an error of 0.01 in the surface reflectance in the UV region results in an AOD error of 0.1 (Veefkinf et al., 2000). In addition, errors in cloud retrieval can also occur, affecting cloud properties such as cloud fraction and optical thickness.

(After the change)

*Li et al. (2012) found that a variation of 0.05 in the surface reflectance in the blue channel can lead to an underestimation of approximately -0.17 in the range where the AOD is less than 0.4. Veefkind et al. (2000) indicated that an error of 0.01 in the surface reflectance in the UV region results in an AOD error of 0.1. Furthermore, **Platnick et al. (2001); Letu et al. (2020)** observed that errors in cloud retrieval can also occur, affecting cloud properties such as cloud fraction and optical thickness*

[References #1]

Kaufman, Y. J., Wald, A. E., Remer, L. A., Gao, B. C., Li, R. R., & Flynn, L. (**1997**). The MODIS 2.1-/spl mu/m channel-correlation with visible reflectance for use in remote sensing of aerosol. IEEE transactions on Geoscience and Remote Sensing, 35(5), 1286-1298.

[References #2]

De Smedt, I., Theys, N., Yu, H., Danckaert, T., Lerot, C., Compernolle, S., ... & Veefkind, P. (**2018**). Algorithm theoretical baseline for formaldehyde retrievals from S5P TROPOMI and from the QA4ECV project. Atmospheric Measurement Techniques, 11(4), 2395-2426.

[References #3]

Howlett, C., González Abad, G., Chan Miller, C., Nowlan, C. R., Ayazpour, Z., & Zhu, L. (**2023**). The influence of snow cover on Ozone Monitor Instrument formaldehyde observations. Atmósfera, 37.

[References #4]

Leitão, J., Richter, A., Vrekoussis, M., Kokhanovsky, A., Zhang, Q. J., Beekmann, M., & Burrows, J. P. (**2010**). On the improvement of NO 2 satellite retrievals–aerosol impact on the airmass factors. Atmospheric Measurement Techniques, 3(2), 475-493.

[References #5]

McLinden, C. A., Fioletov, V., Boersma, K. F., Kharol, S. K., Krotkov, N., Lamsal, L., ... & Yang, K. (**2014**). Improved satellite retrievals of NO 2 and SO 2 over the Canadian oil sands and comparisons with surface measurements. Atmospheric Chemistry and Physics, 14(7), 3637-3656.

[References #6]

Mei, L. L., Xue, Y., Kokhanovsky, A. A., von Hoyningen-Huene, W., De Leeuw, G., & Burrows, J. P. (**2014**). Retrieval of aerosol optical depth over land surfaces from AVHRR data. Atmospheric Measurement Techniques, 7(8), 2411-2420.

[References #7]

Chen, L., Wang, R., Han, J., & Zha, Y. (**2021**). Influence of observation angle change on satellite retrieval of aerosol optical depth. Tellus B: Chemical and Physical Meteorology, 73(1), 1-14.

[References #8]

Wang, Y., Yuan, Q., Li, T., Shen, H., Zheng, L., & Zhang, L. (**2019**). Evaluation and comparison of MODIS Collection 6.1 aerosol optical depth against AERONET over regions in China with multifarious underlying surfaces. Atmospheric Environment, 200, 280-301.

[References #9]

Platnick, S., Li, J. Y., King, M. D., Gerber, H., & Hobbs, P. V. (**2001**). A solar reflectance method for retrieving the optical thickness and droplet size of liquid water clouds over snow and ice surfaces. Journal of Geophysical Research: Atmospheres, 106(D14), 15185-15199.

[References #10]

Letu, H., Yang, K., Nakajima, T. Y., Ishimoto, H., Nagao, T. M., Riedi, J., ... & Shi, J. (**2020**). High-resolution retrieval of cloud microphysical properties and surface solar radiation using Himawari-8/AHI next-generation geostationary satellite. Remote Sensing of Environment, 239, 111583.

5. P3 L60: References will be added with respective to the different products of LER.

➔ We have added the relevant references as suggested.The modified parts are as follows: (The previously written parts are in blue and italics, and the newly added/replaced parts are in red and italics.)

(Line 70-72; In Section 1. Introduction)

This is exemplified by the geometry-dependent surface Lambertian-equivalent reflectivity (GLER) ***(Vasilkov et al., 2017; Qin et al., 2019)*** *and the directionally dependent Lambertian-equivalent reflectivity (DLER)* ***(Tilstra et al., 2021, 2023)****.*

[References #11]

Vasilkov, A., Qin, W., Krotkov, N., Lamsal, L., Spurr, R., Haffner, D., ... & Marchenko, S. (**2017**). Accounting for the effects of surface BRDF on satellite cloud and trace-gas retrievals: a new approach based on geometry-dependent Lambertian equivalent reflectivity applied to OMI algorithms. Atmospheric Measurement Techniques, 10(1), 333-349.

[References #12]

Qin, W., Fasnacht, Z., Haffner, D., Vasilkov, A., Joiner, J., Krotkov, N., Fisher, B., and Spurr, R.: A geometry-dependent surface Lambertian-510 equivalent reflectivity product for UV–Vis retrievals–Part 1: Evaluation over land surfaces using measurements from OMI at 466 nm, Atmospheric Measurement Techniques, 12, 3997–4017, (**2019)**.

[References #13]

Tilstra, L. G., Tuinder, O. N., Wang, P., and Stammes, P.: Directionally dependent Lambertian-equivalent reflectivity (DLER) of the Earth's surface measured by the GOME-2 satellite instruments, Atmospheric Measurement Techniques, 14, 4219–4238, (**2021**)

[References #14]

Tilstra, L. G., de Graaf, M., Trees, V., Litvinov, P., Dubovik, O., and Stammes, P.: A directional surface reflectance climatology determined from TROPOMI observations, Atmospheric Measurement Techniques Discussions, 2023, 1–29, (**2023)**.

6. P3 L84-91: The author shows the suggestion of the methods. However, the purpose of this study and importance of study are not included in the Introduction. Please include the purpose of study and also describe the sections.

➔ We acknowledge that the previous explanation for this section was inadequate. In response to your feedback, we have now included the purpose and significance of this study, as well as a detailed explanation of each section at the conclusion of the introduction.

The revised text is provided below : (The previously written parts are in blue and italics, deleted parts are blue and ~~solid lines~~, and the newly added/replaced parts are in red and italics.)

(Line 99-107; In Section 1. Introduction)

Therefore, in this study, we propose, for the first time, the application of the BRDF model to hyperspectral satellite data for more realistic preliminary surface reflectance data. In this study, we focused on 440 nm, which is used as an input from NO_2, clouds, and aerosols. This algorithm consists of two main steps: atmospheric correction, BRDF modeling and BSR retrieval. The purpose of this study is to enhance the accuracy of satellite-derived prior surface reflectance data by addressing BRDF effects through a method that incorporates the strengths of both GLER and DLER while addressing their limitations. This is crucial for improving the reliability of atmospheric and surface property retrievals from hyperspectral satellite data. A detailed description of each step of the proposed algorithm is provided in Section 3. Section 2 covers the data and study area, and Section 4 presents the results and discussion. ~~*A detailed description of each step is provided in Section 3.*~~

7. P4 Please change the order of section. Section 2.1 will be shown after the Section 2.2.

➔ We have revised the relevant sections as suggested. And also, we edited the title of Section 2. (Study area and Materials → Materials and Study area). Thank you for your .

Below, we have included the revised the order of sections for your review. The modified parts are as follows: (*The previously written parts are in blue and italics*, *and the newly added/replaced parts are in red and italics.*)

(Line 108-149; In Section 2. Study area and Materials)

(Before the change)

2. Study area and Materials

2.1. Study area

2.2. Geostationary Environment Monitoring Spectrometer (GEMS)

(After the change)

2. Materials and Study area

2.1. Geostationary Environment Monitoring Spectrometer (GEMS)

2.2. Study area

8. P4 L104: Level-1C → Level 1C (L1C)

➔ We have revised the relevant sections as suggested. Thank you.

9. P4 L110: 'it does not provide an official cloud mask': The GEMS officially provides the cloud product (GEMS CLD). It is confusing to the reader. What is this sentence means?

10. P4 L110-111: For the clear-sky identification, is this study uses the CCP > 1000 hPa, addition to the ECF<0.2 and CCP = 1013hPa? It has advantage of clear-sky identification from falsely detected as cloudy pixels. However, how about the cloud conditions in real, but cloudy from GEMS CLD?

➔ We think it will be easier for you to understand the answers to the two questions regarding cloud products above if we explain them all at once.

Environmental satellites such as GEMS do not officially provide the cloud detection data that is provided by satellites with multispectral sensors such as MODIS and GK-2A. In this case, cloud detection data is a classification of whether or not clouds are present within a given pixel, often called a "cloud mask". Instead, we utilize a threshold in each output based on variables such as ECF (Effective Cloud Fraction) and CCP (Cloud Centroid Pressure) for classifying as clear-sky and cloud. Therefore, almost GEMS field algorithm use the ECF data to remove these cloud effect, and the threshold varies from 0.2 to 0.4.

The variable CCP indicates the location of clouds, and a CCP value closer to 1013 hPa means the clouds are located closer to the ground. For algorithms that calculate atmospheric aerosols and gases, the effect of clouds close to the ground can be ignored, but for algorithms that calculate ground reflectance, undetected clouds can be a significant source of error.

Therefore, in the quality flag within GEMS CLD ATBD, when ECF is less than 0.2 or CCP is equal to 1013 hPa, it is classified as clear-sky. However, in this study, to remove clouds located very close to the ground, we have set the following criteria: (1) clear-sky if ECF is less than 0.2, and (2) cloud-sky if CCP is more than 1000 hPa, even if ECF is less than 0.2.

We recognize that this sentence may be confusing to other readers, and we have made the following additions and corrections to the text.

We have attached the revised text below. (The previously written parts are in blue and italics, deleted parts are blue and ~~solid lines~~, and the newly added/replaced parts are in red and italics.)

(Line 120-134; In Section 2. Geostationary Environment Monitoring Spectrometer (GEMS))

*The GEMS CLD product is an optical quantity observed at UV-VIS wavelengths, which may differ from the physical properties of real clouds; therefore, it does not provide an official detection data like those from multi-spectral sensors such as MODIS (**Frey et al., 2008**) and GK-2A (Lee and Choi, 2021).~~cloud mask.~~ Cloud detection data, often referred to as a "cloud mask," classifies whether clouds are present within a given pixel. Instead, GEMS utilizes thresholds based on variables such as Effective Cloud Fraction (ECF) and Cloud Centroid Pressure (CCP) to classify pixels as clear-sky or cloudy. Most GEMS field algorithms use ECF data to mitigate cloud effects, with thresholds varying from 0.2 to 0.4. Within the quality flag of GEMS CLD algorithm theoretical basis documents (ATBD) (Choi et al., 2020), pixels are classified as clear-sky when ECF is less than 0.2 or CCP is equal to 1013 hPa. CCP indicates the location of clouds, with values closer to 1013 hPa signifying clouds closer to the ground. While ground-level clouds can be ignored in algorithms calculating atmospheric aerosols and gases, they can significantly affect algorithms calculating ground reflectance.Therefore, in this study, we adopted the following criteria to exclude clouds very close to the ground: (1) pixels are classified as clear-sky if ECF is less than 0.2, and (2) pixels are classified as cloudy if CCP is greater than 1000 hPa, even if ECF is less than 0.2. ~~However, if the effective cloud fraction (ECF) is less than 0.2 and the cloud centroid pressure (CCP) is equal to 1013 hPa, the quality flag in the CLD output indicates a clear sky. However, to mitigate potential errors caused by lower clouds being mistaken as clear-sky, an additional cloud-masking step was performed when the CCP was equal to or greater than 1000 hPa, following the initial masking based on the ECF.~~*

[References #15]

***Frey**, R. A., Ackerman, S. A., Liu, Y., Strabala, K. I., Zhang, H., Key, J. R., & Wang, X. (**2008**). Cloud detection with MODIS. Part I: Improvements in the MODIS cloud mask for collection 5. Journal of atmospheric and oceanic technology, 25(7), 1057-1072.*

[References #16]

***Lee, S., & Choi, J. (2021).** Daytime cloud detection algorithm based on a multitemporal dataset for GK-2A imagery. Remote Sensing, 13(16), 3215.*

[References #17]

***Choi**, Y.-S., Kim, G., Kim, B.-R., Kwon, M.-J., Kim, Y., Yoon, J., won Lee, D., and Kim, J.: Geostationary Environment Monitoring Spectrometer (GEMS) Algorithm Theoretical Basis Document:*

*Cloud Retrieval Algorithm, Tech. rep., Environmental Satellite Center, National Institute of Environmental Research, Ministry of Environment, South Korea, file:///mnt/data/atbd_cld.pdf, version 1.1, Approved by Jhoon Kim on 03 Feb 2021,)(**2020**).*

11. Change "R-value" to 'r'

➔ We have revised the relevant sections as suggested. Thank you.

12. P4 L116-117: The author shows the accuracy of GEMS AOD at 443 nm. However, I am doubtful that this accuracy results is not guaranteed different spectral AOD accuracy. During the spectral conversion of AOD, the error will be enhanced. Why don't the author use the 443 nm AOD values?

➔ As mentioned in the text, most satellite AOD algorithms calculate 550 nm AOD because the 550 nm wavelength is important because it is the most scattered in the atmosphere and is widely used in various chemical models. Therefore, the common reference wavelength for most satellite AOD products is set to 550 nm. The 6SV RTM used to perform the atmospheric correction in this study is also configured to input AOD values at 550 nm. Therefore, the AOD at 550 nm was used as an input in this study.

In the case of the GEMS AOD algorithm, the AOD at 443 nm is first calculated, and then the AOD at 550 nm is determined through wavelength conversion. This process may introduce errors, but no AOD errors due to wavelength conversion have been reported yet in the official GEMS AOD algorithm. However, due to the nature of the 6SV RTM, calculations can only be performed with the AOD at 550 nm as input, limiting the use of the 443 nm AOD.

I agree with your opinion and appreciate your valuable comment. It would be beneficial to conduct an analysis of surface reflectance considering the impact of wavelength conversion in future studies.

13. P5 L125-130: For the supplement of GEMS AOD gap, this study used the CAMS AOD values. However, the CAMS AOD have significant biases as compared to the GEMS AOD. The AOD bias between GEMS and CAMS will be affected to the discontinuous spatial distribution of AOD, and thus affecting to the surface reflectance calculation. How much this bias affecting the surface reflectance estimation? In addition, how did this study correct the AOD bias between CAMS and GEMS?

➔ We fully acknowledge that there are differences between CAMS AOD data and GEMS AOD data, and we agree with this observation. However, this study is a foundational effort to develop a working algorithm for calculating surface reflectivity (BSR) using GEMS satellite data. The additional use of CAMS AOD data was designed to enhance the accuracy of the reflectivity product and ensure the stability of the calculations.

When comparing CAMS AOD and GEMS AOD, we observed an RMSE difference of approximately 0.2, with GEMS tending to underestimate. When calculating TOC based on this data, the RMSE was about 0.015. Given that CAMS AOD data was used in a relatively small proportion of the pixels for BRDF modeling, we determined that this influence could be sufficiently mitigated. Despite the inherent differences between GEMS AOD and CAMS AOD data, we prioritized maintaining a complete dataset over potential biases.

Furthermore, qualitative analysis using CAMS AOD in the absence of GEMS AOD, prior to applying the algorithm, revealed no noticeable discontinuities, supporting the applicability of this method.

As the reviewer pointed out, we recognize that the AOD bias between the two datasets affects TOC, and this influence is subsequently transferred to BSR. However, it is important to emphasize that this study aims to develop a methodology for the current GEMS algorithm's surface reflectance calculation. While acknowledging the limitations of not addressing the bias between the GEMS and CAMS AOD datasets, this study provides a fundamental framework for operational use. Future research will focus on developing and integrating bias correction techniques to further improve calculation accuracy.

By transparently addressing these limitations and outlining plans for future improvements, we demonstrate our commitment to enhancing the reliability and precision of surface reflectance calculations from satellite data. The limitations of this aspect have been included in the final discussion section, and the last section, originally titled "Conclusion," has been revised to "Conclusion and Discussion."

We have attached the revised text below. (The previously written parts are in blue and italics, deleted parts are blue and ~~solid lines~~, and the newly added/replaced parts are in red and italics.)

(Line 466-482; In Section 5.Conclusion and Discussion)

(Before the change)

In conclusion, our study demonstrated that BSR can effectively simulate realistic reflectance, surpassing the minimum reflectance approach used in many existing studies. Although limitations exist, such as the challenge of capturing sudden changes in surface characteristics such as snow or ice cover, our research is pioneering in its application to BRDF modeling and evaluation in hyperspectral observation satellite studies. By combining the high temporal and spatial resolution of GLER with the BRDF considerations of DLER, we laid the foundation for improved accuracy in the AQ output. Our findings suggest that the utilization of BSR, a dataset reflecting realistic reflectance with BRDF effects, can enhance various climate analysis studies, marking a significant advancement in the field.

(After the change)

Although limitations exist, such as the challenge of capturing sudden changes in surface characteristics such as snow or ice cover. And also, To inhance stability, we designed a method to use CAMS AOD data in the absence of GEMS AOD, acknowledging the presence of some bias. Despite this limitation, we prioritized maintaining a stable dataset. Our research is pioneering in its application to BRDF modeling and evaluation in hyperspectral observation satellite studies. We are committed to further refining our approach and will strive to address these biases in future research to improve calculation accuracy.

In conclusion, our study demonstrated that BSR can effectively simulate realistic reflectance, surpassing the minimum reflectance approach used in many existing studies. By combining the high temporal and spatial resolution of GLER with the BRDF considerations of DLER, we laid the foundation for improved accuracy in the AQ output. Our findings suggest that the utilization of BSR, a dataset reflecting realistic reflectance with BRDF effects, can enhance various climate analysis studies, marking a significant advancement in the field.

14. Section 3: Before beginning the section 3, the author needs to the definition and calculation process of Top-of-Canopy from GEMS.

➔ We recognized the lack of mention of this part and have added TOC-related sentences to the text.

We have attached the revised text below. (The previously written parts are in blue and italics, deleted parts are blue and ~~solid lines~~, and the newly added/replaced parts are in red and italics.)

(Line 170-174; In Section 3. Background Surface Reflectance (BSR) retrieval algorithm)
Figure 1 depicts a comprehensive flow chart of the BSR retrieval algorithm, which comprises two primary steps: (1) atmospheric correction and (2) BRDF modeling and BSR retrieval. The top-of-canopy (TOC) reflectance from GEMS represents the actual surface reflectance derived through atmospheric correction when AOD, CLD, and O3T products are available. To evaluate the applicability of the BSR derived in this study, validations were performed against the GEMS TOC ~~Top-of-Canopy (TOC)~~ data as reference data.

15. P5 L147 what is the 'traditional minimum reflectivity method'? Please add the details and references.

➔ The "minimum reflectance method," referred to in the text as the traditional minimum reflectivity method, is an algorithm that currently underpins various LER data. This method was first designed for the Total Ozone Mapping Spectrometer (TOMS) and was initially mentioned in the study by Eck et al. (1987). It involves selecting and using the minimum value among the surface reflectances observed over a certain period for each grid area. This approach effectively reduces the influence of temporary air pollution (such as aerosols and clouds) on the reflectivity measurements, thereby isolating the true surface reflectance.

$$R = \frac{A - A_0(\tau, \theta_0, \theta, \phi)}{f_1(\tau, \theta_0) f_2(\tau, \theta) + [A - A_0(\tau, \theta_0, \theta, \phi)] f_3(\tau)}$$

equation 1. Lambertian Equivalent Surface Reflectance (LER) calculation formula

It can be calculated using the above formula, and the minimum value among these calculated values is selected. Where A is the directional albedo, A_0 is the atmospheric albedo, and f_1, f_2, f_3 are fractions accounting for various scattering effects.

Therefore, references to this paper and the GLER and DLER papers that have recently been calculated based on this algorithm (**Eck et al., 1987**) have been added to the text. However, the word "traditional" was deleted from the text to avoid confusing readers with different algorithms.

Below is the edited text. (The previously written parts are in blue and italics, deleted parts are blue and ~~solid lines~~, and the newly added/replaced parts are in red and italics.)

(Line 174-176; In Section 3. Background Surface Reflectance (BSR) retrieval algorithm)
*Additionally, a comparison was made with the LER data generated using the ~~traditional~~ minimum reflectivity method which is used for a variety of LER datasets **(Kleipool et al. (2008); Koelemeijer et al. (2003); Tilstra et al. (2017))** and was first introduced in the work of **Eck et al. (1987).***

[References #18]

Kleipool, Q. L., Dobber, M. R., de Haan, J., & Levelt, P. F. (**2008**). Earth surface reflectance climatology from 3 years of OMI data. Journal of Geophysical Research: Atmospheres, 113(D18).

[References #19]

Koelemeijer, R. B. A., De Haan, J. F., & Stammes, P. (**2003**). A database of spectral surface reflectivity in the range 335–772 nm derived from 5.5 years of GOME observations. Journal of Geophysical Research: Atmospheres, 108(D2).

[References #20]

Tilstra, L. G., Tuinder, O. N. E., Wang, P., & Stammes, P. (**2017**). Surface reflectivity climatologies from UV to NIR determined from Earth observations by GOME-2 and SCIAMACHY. Journal of Geophysical Research: Atmospheres, 122(7), 4084-4111.

[References #21]

Eck, T. F., Bhartia, P. K., Hwang, P. H., & Stowe, L. L. (**1987**). Reflectivity of Earth's surface and clouds in ultraviolet from satellite observations. Journal of Geophysical Research: Atmospheres, 92(D4), 4287-4296.

16. Figure 1: Change the caption to "Flowchart of GEMS BSR algorithm."

➔ We have revised the relevant sections as suggested. Thank you.

17. Equation 1-5 and related sentences: For the equation writing, please use the subscript. All the equation variables are not use the subscript and it may confusing to the equation. In addition, all the equation variables will be clarify in the manuscript.

➔ We have revised the relevant sections as suggested. Additionally, when variables written as formulas are mentioned in the text, they are written in italics, the same as the formula.

Below, we have included the revised text and the updated figure for your review. The modified parts are as follows: (The previously written parts are in blue and italics, and the newly added/replaced parts are in red and italics.)

(Line 189-193; In Section 3.1. Atmospheric correction)

By employing the three atmospheric correction coefficients (xap, xb, and xc) derived from the 6SV RTM, the TOC reflectance can be calculated from the TOA reflectance. The surface reflectance was then calculated from the TOA reflectance, as expressed in Equation (1). The atmospheric correction coefficients xap, xb, and xc can be computed using Equations (2), (3), and (4), where they represent the inverse of the transmittance, scattering term of the atmosphere, and spherical albedo, respectively.

(Line 223-226; In Section 3.2 BSR retrieval through BRDF modeling)

The Roujean BRDF model defines surface reflectance as a combination of isotropic, geometric, and volumetric scattering components. It comprises two physical kernels (f_1 and f_2) and three empirical coefficients (K_0, K_1, K_2; BRDF parameters) that describe the mechanism of each component, as shown in Equation 5.

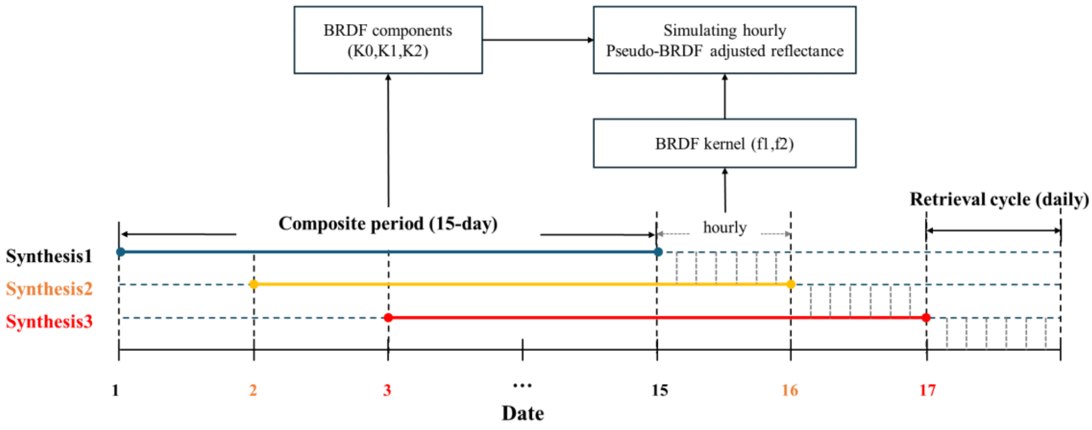

Figure 1. Schematic of 15-day composite period and retrieval cycle for BRDF modeling (Figure 2 in this article; Before the change)

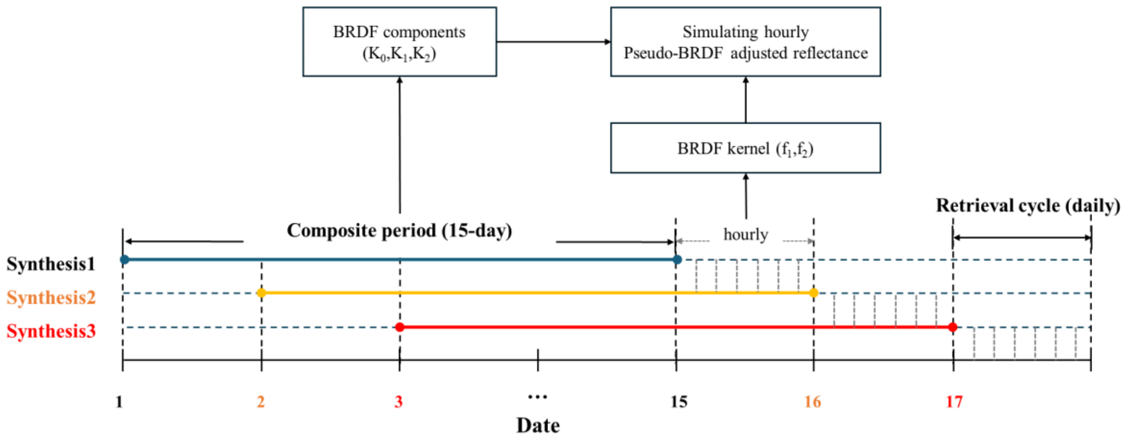

Figure 2. Schematic of 15-day composite period and retrieval cycle for BRDF modeling (Figure 2 in this article; After the change)

18. P6 L160: For the 6SV RTM, How to adopting the spectral response function of GEMS?

➔ *As mentioned in line 188 of the text (in article), the 6SV is calculated by dividing it into 2.5 nm intervals and summing the values afterwards. Therefore, for GEMS with a band width of 3.6 nm for one channel, we calculated it with a monochromatic wavelength value (center wavelength).*

*In addition, the LUTs for calculating the reflectance of the ground surface of other current satellites (TROPOMI and GOME-2 DLER) are mostly calculated at monochromatic wavelengths. Below are the papers of GOME-2 (**Tilstra et al., 2021**) and TROPOMI (**Tilstra et al., 2023**) DLER algorithms mentioned in this study, both of which are mentioned in table1.*

*** Tilstra et al., 2021 : Same as [References #13 in this response letter]**
*** Tilstra et al., 2021 : Same as [References #14 in this response letter]**

19-1 Table 1: For the Aerosol type, what is “continental”? Do you have any detailed aerosol optical and physical properties, or related references?

➔ The “Continental” model utilized in this study is an aerosol model predefined within 6SV. The term "Continental" in the context of aerosol types refers to aerosol particles typically found in continental regions. This is a model produced by mixing three basic components: dust-like component (DUST), water-soluble component (WATE), and soot component (SOOT). The weighted averages of DUST, WATE, and SOOT in that order are 0.7 and 0.29, 0.01, respectively.

For the continental aerosol model, the manual specifies the following properties based on predefined components and their volume mixing ratios:

(1) Dust-Like Component (D.L.):
Volume Concentration: 113.98352 $\mu m^3/cm^3$
Particle Number Concentration: 54.734 $part/cm^3$
Characteristics: Coarse mode particles with significant scattering properties.

(2) Water-Soluble Component (W.S.):
Volume Concentration: 113.98352×10^{-6} $\mu m^3/cm^3$
Particle Number Concentration: 1.86850×10^{6} $part/cm^3$
Characteristics: Fine mode particles, often hygroscopic, affecting scattering and absorption.

(3) Oceanic Component (O.C.):
Volume Concentration: 5.14441 $\mu m^3/cm^3$
Particle Number Concentration: 276.0500010 $part/cm^3$
Characteristics: Typically sea salt particles, contributing to scattering.

(4) Soot Component (S.C.):
Volume Concentration: 59.777553×10^{-6} $\mu m^3/cm^3$
Particle Number Concentration: 1.86850×10^{6} $part/cm^3$
Characteristics: Strongly absorbing particles, influencing the single scattering albedo.

These properties and their computational parameters are discussed in the context of aerosol models in the 6S Manual, especially within the sections describing the aerosol optical properties, phase functions, and the mixing of different aerosol types based on the volume percentages(detailed in 6SV Manual Part2 (Vermote et al., 2006)).

[Reference #22]
Vermote, E., Tanré, D., Deuzé, J. L., Herman, M., Morcrette, J. J., & Kotchenova, S. Y. (2006). Second Simulation of a Satellite Signal in the Solar Spectrum - Vector (6SV) User Guide (Version 3). University of Maryland, Laboratoire d'Optique Atmosphérique, European Centre for Medium Range Weather Forecast. Retrieved from 6S_Manual_Part_1, 6S_Manual_Part_2, 6S_Manual_Part_3.

19-2. In addition, the TCO value range is too narrow. In East Asia, the total ozone is ranged from 200-600 DU based on the daily data. 250-350 DU ranges are too narrow. Do this narrow TCO range affect the surface reflectance retrieval?

➔ The range and interval settings of TCO when creating the LUT were heavily reliant on criteria from other satellites. Both COMS (**Lee et al., 2018**) and GK-2A (**Lee et al., 2020**), a geostationary satellite focused on observations over Asia like GEMS, land surface reflectance algorithm utilized the same TCO for LUT generation as our study.

Additionally, based on the findings of **Shin et al. (2021),** we confirmed that most of the ozone over East Asia is distributed within the range of 250-350 DU. This paper analyzed the trend of TCO from 1997 to 2017, with **Figure 1** in the paper illustrating the results.

While ozone levels can reach up to 600 DU, this study is a preliminary investigation for the application of the algorithm in the field. Therefore, the LUT was created with a focus on the efficiency of the calculations..

[Reference #22]
Lee, C. S., Han, K. S., Yeom, J. M., Lee, K. S., Seo, M., Hong, J., ... & Roujean, J. L. (**2018**). Surface albedo from the geostationary Communication, Ocean and Meteorological Satellite (COMS)/Meteorological Imager (MI) observation system. GIScience & Remote Sensing, 55(1), 38-62.

[Reference #23]
Lee, K. S., Chung, S. R., Lee, C., Seo, M., Choi, S., Seong, N. H., ... & Han, K. S. (**2020**). Development of land surface albedo algorithm for the GK-2A/AMI instrument. Remote Sensing, 12(15), 2500.

[Reference #24]
Shin, D., Oh, Y. S., Seo, W., Chung, C. Y., & Koo, J. H. (**2021**). Total ozone trends in east asia from long-term satellite and ground observations. Atmosphere, 12(8), 982.

20. P9 L231: This study uses the 15-day period for the clear-sky identification. However, 15-day is too narrow temporal window. From the below reference, the 30-day temporal window is essential to identify the clear-sky conditions. Park, S. S., Yu, J. E., Lim, H., and Lee, Y. G.: Temporal variation of surface reflectance and cloud fraction used to identify background aerosol retrieval information over East Asia, Atmos. Environ., 309, 119916.

➔ The synthesis period for BRDF (Bidirectional Reflectance Distribution Function) modeling in this study was set to 15 days, as it was empirically determined to be optimal. The same period was applied for LER (Lambertian Equivalent Reflectance) calculation.

The referenced paper (**Park et al., 2023**) also employs the minimum reflectance method, which selects the minimum value within a grid over a given time window. They analyzed synthesis period settings of 15, 20, 30, and 40 days. The findings suggest that a 30-day temporal window is generally recommended for identifying clear-sky conditions due to cloud cover variability. However, the study also highlights the importance of considering surface reflectance variability when choosing the temporal window. It concludes that a 15-day window can effectively balance minimizing cloud contamination and maintaining consistent surface reflectance, as longer windows reduce cloud influence but increase surface reflectance variability.

Therefore, we determined that the 15-day compositing window set in this study is appropriate for both the accuracy of BRDF modeling and the mitigation of errors introduced by clouds when generating LERs.

Through the paper you mentioned, we were able to obtain a scientific basis for the 15-day synthesis period set in this study. We sincerely appreciate your guidance in this matter. Consequently, we have added the referenced paper to the main text and made the necessary modifications. Thank you once again for your valuable feedback.

The revised section is attached below. The modified parts are as follows: (The previously written parts are in blue and italics, and the newly added/replaced parts are in red and italics.)

(Line 261-267; In Section 3.3. GEMS LER assumption)
(Before the change)
The "GEMS LER" was determined as the minimum reflectance over a 15-day period, aligning with the BRDF synthesis period. Additionally, the GEMS LER was used for further gap filling in cases of persistent missing in GEMS BSR, despite utilizing the age variable.

(After the change)
*The "GEMS LER" was determined to be the minimum reflectance over a 15-day period to match the BRDF synthesis period. A 15-day synthesis period was also found by **Park et al. (2023)** to be an effective balance between minimizing cloud contamination and maintaining consistent surface reflectance in the application of the minimum reflectance method. The resulting GEMS LER was used for additional gap filling in cases where the GEMS BSR was consistently missing despite utilizing the age variable.*

[Reference #25]
Park, S. S., Yu, J. E., Lim, H., & Lee, Y. G. (**2023**). Temporal variation of surface reflectance and cloud fraction used to identify background aerosol retrieval information over East Asia. Atmospheric Environment, 309, 119916.

21. Figure 3: The intercomparison has been done by using the GEMS TOC. By the comparison with GEMS TOC, how to be explain the significance of accuracy improvements?

➔ As mentioned in the introduction, using LER based on the minimum reflectance method as an alternative reflectance causes an underestimation of surface reflectance, leading directly to the overestimation of AOD and affecting other L2 products such as clouds and gas products.

Both BSR and LER are meaningful variables that have already simulated values almost similar to TOC reflectance, in advance.

As highlighted in section 4.2.2, "Surface Reflectance Influence on AOD Variability in Cropland and Urban Areas," while the overall accuracy improves by approximately 3%, the impact on AOD shows that BSR is up to about 10% more accurate than LER, especially in urban areas during winter.

Therefore, the enhancement of BSR is significant as it addresses the inherent issues associated with LER.

22. P11 L275: GEMS SFC is not defined in this manuscript.

➔ SFC stands for Surface Reflectance, which in this study is synonymous with TOC (Top-Of-Canopy) Reflectance. However, for consistency throughout the paper, we have changed it to TOC Reflectance. Thank you.

23. P13 L299: Please add the references and detailed products used in this study.

➔ The analysis was conducted based on MODIS land cover data. The data used is from the MODIS/Terra+Aqua Land Cover Type Yearly L3 Global 0.05Deg CMG V061 (MCD12C1) (**Strahler et al.,1994**), specifically from the year 2021. We used the land cover according to the IGBP classification within the MODIS Land Cover data. The values for the four land cover types used in this study are Grassland, Cropland, Shrubland and Urban. The average values for all four land cover types were utilized.

We acknowledged that this explanation was insufficient and additionally mentioned the MODIS land cover datasets as follows. (The previously written parts are in blue and italics, and the newly added/replaced parts are in red and italics.)

(Line 333-336; In Section 4.2.1. Time series consistency analysis by land types)
*To assess the simulation performance based on the time series of the BSR, we analyzed the time series stability across four land types (grassland, cropland, shrubland, and urban) using MODIS land cover data. The dataset utilized in this study is derived from the MODIS/Terra+Aqua Land Cover Type Yearly L3 Global 0.05Deg CMG V061 (MCD12C1) product (**Strahler et al.,1994**). The classification follows the International Geosphere-Biosphere Programme (IGBP) scheme within the MODIS Land cover dataset. Specifically, we employed the land cover data from the year 2021*

[Reference #26]

Strahler, A., Moody, A., Lambin, E., Huete, A., Justice, C., Muller, J., Running, S., Salomonson, V., Vanderbilt, V., and Wan, Z.: MODIS land cover product: Algorithm theoretical basis document, MODIS documentation, (**1994)**

24. P15 L315: From Table 1, the AOD bin range is not exceeded to 1.5. How to be analyzed the AOD ranges up to 2.0?

➔ AOD values above 1.5 were changed to 1.5 and calculated, but were marked as bad quality with their own quality flag and not used as input for analysis and BRDF modeling. AOD above 1.5 is not only rare, but other satellites such as VIIRS and GOES-R currently define 0.8 and above as a high AOD condition. In addition, according to the validation report of the SEVIRI AOD algorithm (CM SAF, 2017), the SEVIRI satellite also specified a maximum value of 1.5 for AOD in its reflectance calculation (As shown in the Figure 3).

[Reference #27]

Clerbaux, N.; Ipe, A.; De Bock, V.; Urbain, M.; Baudrez, E.; Velazquez-Blazquez, A.; Akkermans, T.; Moreels, J.; Hollmann, R.; Selbach, N. **CM SAF** Aerosol Optical Depth (AOD) Data Record–Edition 1. Satell. Appl. Facil. Clim. Monit. **2017**, doi:10.5676/EUM_SAF_CM/MSG_AOD/V001.

Table 2 : Values used in the LDA LUTs

Parameters and unit		Values used for RTM simulations
AOD	Aerosol Optical Depth at 550nm (unit less)	0.05 0.1 0.15 0.2 0.3 0.4 0.5 0.6 0.7 0.8 0.9 1.0 1.25 1.5
k	RPV parameter controlling the bowl/bell shape (Minnaert function) (unit less)	0.3 to 1.0 by step of 0.05
theta	RPV parameter controlling the forward/backward scattering (unit	-0.35 to 0.05 by step of 0.05

Figure 3. AOD values used in SEVIRI AOD algorithm (CM SAF, validation report (2017))

25. Figure 8: Is it possible to include the direct comparison between GEMS BSR and LERs?

➔ Figure 8 (in this article) presents a comparison between TOC (the reference data in this study) and GEMS BSR, OMI GLER, and TROPOMI DLER data. And also, Figure 9 (in this article) shows a comparison of BSR with GLER and BSR with DLER.

These figures are attached below (Fig1 and Fig 2 in this letter).

However, to prevent any confusion regarding the order, a brief explanation of the figures has been added before discussing Figures 8 and 9 in the text.

The edited parts are as follows: (The previously written parts are in blue and italics, and the newly added/replaced parts are in red and italics.)

(Line 411-412; In Section 4.4. Intercomparison between BSR and LER database)
Figure 8 compares GEMS TOC with GEMS BSR, TROPOMI DLER, and OMI GLER. Figure 9 presents the intercomparison between BSR and OMI GLER, as well as BSR and TROPOMI DLER.

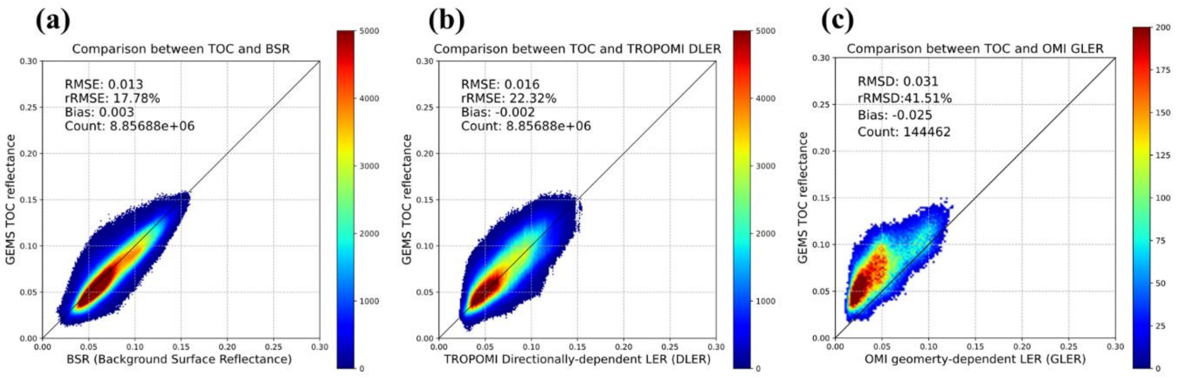

Fig 1. Figure 8 in this article (Distribution density plot of GEMS BSR, TROPOMI DLER, and OMI

GLER based on GEMS TOC observations. (a) GEMS BSR; (b) TROPOMI DLER; (c) OMI GLER)

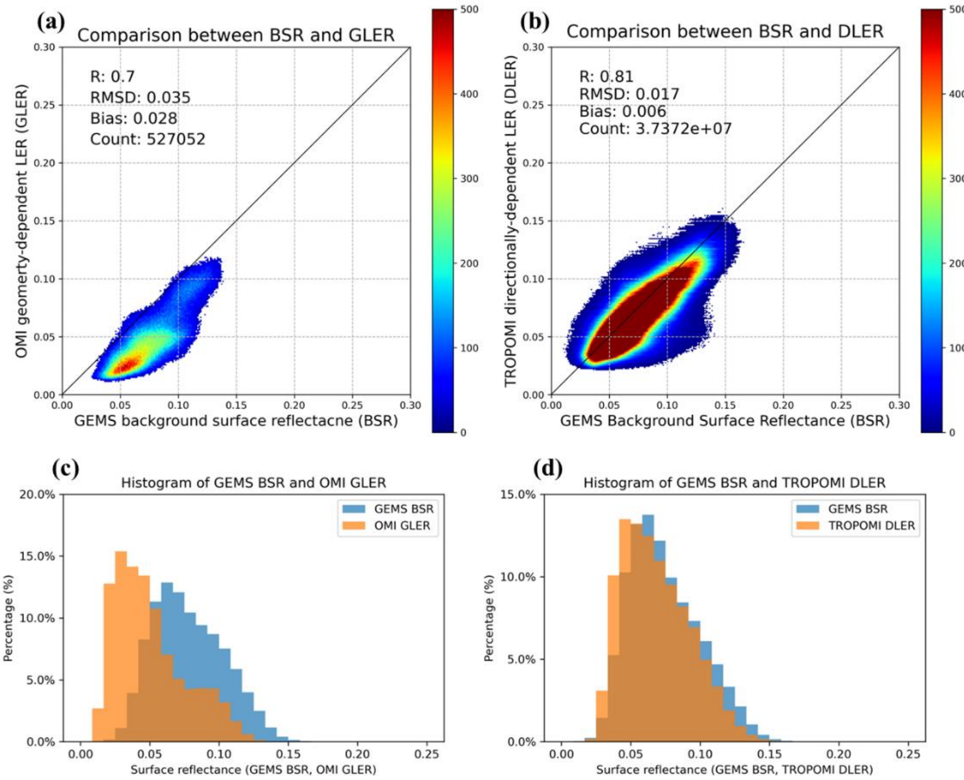

Fig 2. Figure 9 in this article (Quantitative comparison of GEMS BSR, TROPOMI DLER, and OMI GLER value distributions (a) Density plot of BSR and GLER; (b) Density plot of BSR and DLER; (c) Histogram of BSR and GLER; (d) Histogram of BSR and DLER)